J. Min. Metall. Sect. B-Metall. 57 (3) (2021) 389 - 400

Journal of Mining and Metallurgy, Section B: Metallurgy

AN EFFICIENT AND ENVIRONMENTALLY FRIENDLY ROUTE FOR PbS CRYSTAL RECOVERY FROM LEAD ASH GENERATED IN TIN REMOVAL SECTION (LATR) VIA HIGH-SPEED LEACHING AND RECRYSTALLIZATION METHOD

Y.-K. Feng [a,b], X.-Q. Peng [a], H.-H. Shi [a], W. Zhang [a,c,d,e*], Q.-T. Zuo [b,c,d,e#]

[a] School of Ecology and Environment, Zhengzhou University, Zhengzhou, Henan, P. R. China
[b] School of Water Conservancy Engineering, Zhengzhou University, Zhengzhou, Henan, P. R. China
[c] Henan International Joint Laboratory of Water Cycle Simulation and Environmental Protection, Zhengzhou, P. R., China
[d] Zhengzhou Key Laboratory of Water Resource and Environment, Zhengzhou, China
[e] Yellow River Institute for Ecological Protection and Regional Coordination Development, Zhengzhou University, Zhengzhou, Henan, P. R. China

(Received 08 March 2020; accepted 19 July 2021)

Abbreviation/acronym/symbol full form

Abbreviation/acronym	Symbol full form
LATR	Lead ash generated in Tin removal section
$Pb_{in\ the\ LATR}$	The Pb element in original LATR used in the leaching process
$Pb_{in\ the\ filtrate}$	The Pb ions in the filtrate after leaching process

Abstract

This paper mainly investigated the synthesis of a high purity PbS crystal directly from lead ash which was collected from Tin ash removal process (LATR). The LATR was firstly disposed by nitric acid leaching system to generate the lead nitrate solution. The PbS crystal was prepared by mixing the lead nitrate solution with the sodium sulfide at the room temperature (25 °C). The effects of molar ratio of HNO_3 to $Pb_{in\ the\ LATR}$ on Pb leaching efficiency was investigated, demonstrating that the Pb leaching efficiency could attain to 82.9 % at molar ratio of 3. The leaching ratio of As, Cu, Fe, and Al generally increased with increasing molar ratio of HNO_3 to $Pb_{in\ the\ LATR}$, while 99.99 wt% of Sn was still left in the residue. In the process of generating PbS crystal from the leaching solution, the yield of PbS crystal increased with increasing molar ratio of Na_2S to $Pb_{in\ the\ filtrate}$. The yield of PbS crystal could up to 93.1% at a molar ratio of 1.5. Overall, this method proved to be an efficient and environmental friendly route for synthesis of high quality PbS crystal directly from the common lead containing waste from the lead ore or secondary smelting factory.

Keywords: *Lead ash; PbS crystal; Leaching; Recrystallization; Recovery; Environmentally friendly*

1. Introduction

China is producing and consuming a large quantity of lead in the world every year, and more attention has also been paid to the lead pollution. In the lead smelting enterprise, many lead alloys are refined and generated every day in huge amount, including tin-lead alloy, antinomy-lead alloy, nickel-lead, cobalt-lead, zinc-lead alloy, and calcium-lead alloy [1-5]. Most of lead elements are refined (at a higher temperature) and finally enter into the lead alloy product [6, 7]. However, we should not ignore the fact that a large quantity of by-products is generated in the smelting process. The typical by-products mainly include lead ash and lead slag. The lead ash is usually generated and emitted into the factory dust collector, and the lead slag is generated during the smelting-cooling process of the lead compounds [8-10]. The lead ash is quite common in the lead smelting enterprise in a relatively large quantity [11-14]. As reported, the annual production of lead ash can reach up to nearly 50,000 tons [15].

*Corresponding author: zhangwei88@zzu.edu.cn *; zuoqt@zzu.edu.cn #*

https://doi.org/10.2298/JMMB200308035F

Currently, most of lead ash is directly circled into the melting process (in the furnace). This smelting process is usually conducted at a higher temperature, and it can easily emit large amount of lead particles [16]. Besides the smelting process, a hydro-electrometallurgy route is also applied in the recycling of fly ash generated in spent lead acid battery smelting process [17]. In the hydro-electrometallurgy route, the chemical reagents, e.g. HNO_3 or NaOH, are used to leach the fly ash, and then the pregnant leach solution after leaching is electrodeposited to get lead dioxide and metallic lead on the anode and cathode, respectively. The above hydro-electrometallurgy approach is beneficial of production of high purity lead product, but its higher energy consumption in this process should not be ignored. The composition of lead fly ash is similar to the spent lead paste, for their main components are lead oxide or lead sulfate. Thus, the method for recycling spent lead paste should also be a reference to the treatment of lead fly ash, such as the reagent dissolution- electrowinning method, the leaching by citric acid solution method, and the desulfurization- dissolution- electrowinning method [18-20].

It would be quite attractive to explore an efficient and feasible method for recycling the lead ash. For different sections where the lead ash is produced in the lead ore or secondary, the composition of lead ash can also be different. Besides the Pb element, the lead fly ash also consists of other metal compound e.g. antinomy, nickel, cobalt, iron, copper, and aluminum, et al. The lead compound in the fly ash usually consists of lead, lead oxide, lead sulfide, lead sulfate, and oxysulfates ($PbO{\cdot}PbSO_4$ or $(PbO)_2{\cdot}PbSO_4$) [21,22]. Currently, more attention is paid to the recycling of spent lead waste (including spent lead paste, lead sludge, and lead fly ash) to generate lead oxide products. However, the lead oxide product should not be the single choice for generating Pb products, other lead compound (such as PbS and $PbCl_2$) should also be an ideal choice [23, 24]. Considering the special composition of LATR, the PbS could also be an alternative product (generated from LART) for it could simplify the recycling process. It is obvious that the simpler recycling process could reduce the emission of lead containing particles into outside environment.

The proposed schematic diagram of this study could be illustrated by Fig. 1. As shown, this study was mainly focused on two key issues. Firstly, the LATR was leached by the nitric acid, where the lead element was entered into the filtrate ($Pb_{\text{in the filtrate}}$), while the majority of impurity element was left in the filter cake due to their attachment between the impurity compound and the residue. Secondly, the generated filtrate was mixed and then it reacted with sodium sulfide to generate PbS crystal (namely the crystallization process). This study had a positive significance for LATR recovery and preparation of high purity lead sulfide crystal.

2. Material and Methods

2.1. Raw materials and Reactants

The LATR used in this experiment was collected from the tin element removing section (an essential process to refine the tin - lead alloy), applied by Hubei Jinyang Metallurgical Co., Ltd. The concentrations of main elements including Pb, Sn, As, Fe, Cu, and Al were determined and shown in Fig. 2(b), and the detailed process for determination of the main elements was presented in Supporting Information. It was obvious that the major elements in the original LATR were Pb (81.4%) and Sn (7.2%), also with small amount of As, Fe, Cu, and Al. The XRD pattern of original LATR was shown in Fig.2 (c), also illustrating the main crystal composition in the LATR was PbO and SnO_2. From the appearance (Fig. 2(a)) of the original LATR, the collected LATR was yellow powder, mainly due to the existence of PbO crystal. As shown in the SEM image (Fig. 2(d)), the LATR was with irregular sphere and rough porous surface.

The nitric acid used in this study was of analytical purity, supplied by Yantai Shuangshuang Chemical Co., Ltd. The sodium sulfide was also of analytical purity, purchased by Tianjin Damao Chemical Reagent Co., Ltd. The standard solution of Al, Fe, and Cu was supplied by National Nonferrous Metals Research Institute.

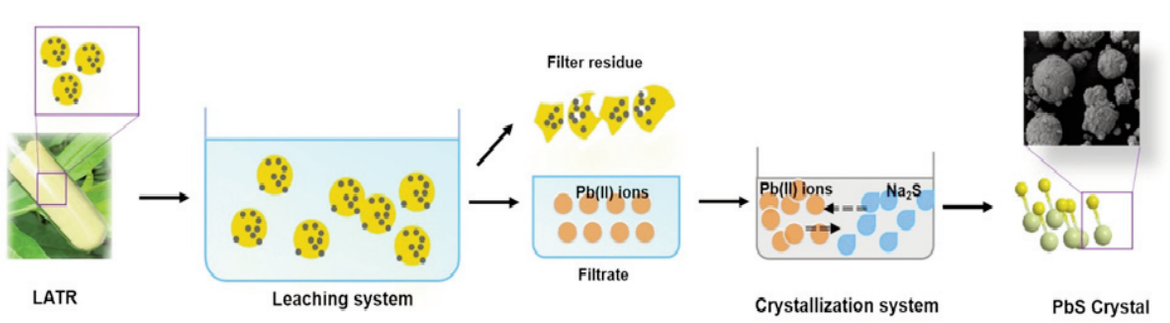

Figure 1. *Proposed schematic diagram for this study*

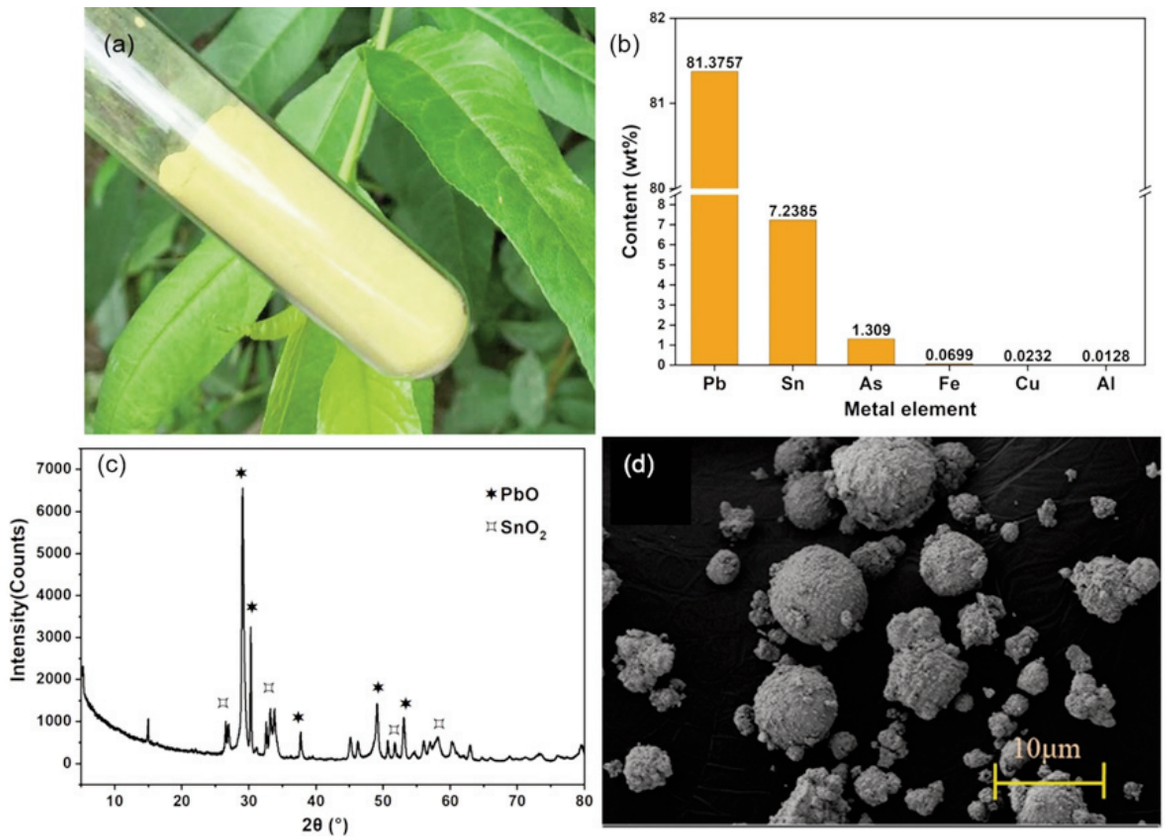

Figure 2. *The characterization of the original LATR: (a) the appearance of LATR packed in the test tube; (b) the concentration of main metal elements in LATR samples; (c) The XRD pattern of original LATR; (d) The SEM image of LATR with Mag of 1 kX*

2.2. Leaching of LATR

To study the leaching efficiency of LATR in nitric acid system, various concentrations of nitric acid (0.6, 0.8, 1.0, and 1.2 mol/L, in Table S1) were separately mixed up with 50 g of LATR in 1L beaker at 25 °C with a stirring speed of 400 rpm (Figure S1).

During the leaching process, the solution sample (10 mL) was quickly withdrawn from the mixed solution in the beaker at setting leaching time of 0, 10, 20, 30, 60, 90, and 120 minutes, respectively. The withdrawn solution samples were then directly filtrated through the microporous membrane (0.45μm pore size). The concentration of lead in the filtrate was measured by the EDTA-2Na Testing Method (explained in SI). The concentrations of Sn, As, Cu, Fe, and Al were determined by ICP-OES 5100 (Keysight Technologies).

At the end of leaching time (120 minutes), the left mixed slurry was filtered to get the filtrate for the next step. The residual filter cake was continuously washed with deionized water until the pH of washing water was near to 7, followed by drying in the oven under 55 °C for 24 hours. The concentrations of Pb, Sn, As, Cu, Fe, and Al in the filtrate and residual filter cake were measured to analyze the flow of main elements during the leaching process.

The leaching efficiency of lead and other elements was calculated by Eq. (1).

$$\textit{Leaching efficiency}\ (wt\%) = v_1 \times m_1 / (g_1 \times w_1) \times 100\% \quad (1)$$

Here, v_1 stands for total volume of leaching experiment (L); m_1 stands for mass concentration of metal ions (g/L); g_1 stands for the weight of LATR (g); and w_1 stands for the percentage of metal element in LATR (wt%).

2.3. Synthesis of PbS crystal

Various mass of sodium sulfide reagents was separately added into the stored filtrate solution in 250 mL tall beaker under 25 °C for 30 minutes (as shown in Figure S1). The added amount of sodium sulfide reagents was calculated according to various molar ratio of Na_2S to $Pb_{\text{in the filtrate}}$ as 0.75, 1, 1.25 and 1.5, respectively (as shown in Table S2).

At the reaction end of 30 minutes, the solution after reaction was quickly filtered, then the solid filter

cake was washed by deionized water, and finally dried in the oven under 55 °C. The conversion rate of Pb (wt%) at various molar ratio of Na_2S to $Pb_{in\ the\ filtrate}$ could be calculated by Eq. (2).

$$The\ conversion\ rate\ of\ lead\ (wt\%) = g_2 \times w_2 / (m_2 \times v_2) \times 100\% \quad (2)$$

In the Eq. (2), g_2 represents the mass of the synthesis product (g); w_2 represents the content of lead in the synthesized product (wt%); m_2 represents the concentration of lead in the stored filtrate solution (g/L); and v_2 represents the volume of the stored filtrate solution (L).

2.4. Characterization of Original LATR and PbS crystal products

The original LATR and synthesized PbS crystal were both investigated by X-ray Powder Diffraction method (Philips, PANalytical B.V., Holland) with Cu Kα radiation (λ = 1.54 Å), while the XRD patterns were calculated through the X'pert Highscore Software.

The micromorphology for original LATR and prepared PbS crystal was investigated through Focused Ion Beam Scanning Electron Microscopy (Zeiss/Auriga FIB SEM).

2.5. Thermodynamics analysis of lead and other metal elements in the solution

The Potential-pH phase diagram and Fraction diagram for Pb, Sn, As, Cu, Fe, and Al were calculated by the MEDUSA software, which has been commonly used in thermodynamics analysis [25-27].

3. Results and Discussion

3.1. Leaching of LATR

The leaching efficiency of lead from the LART with varying molar ratio of HNO_3 to $Pb_{in\ the\ LART}$ was presented in Fig. 3. As shown in Fig. 3, the leaching efficiency of lead increased quickly at leaching time ranging from beginning to 20 minutes. After 20 minutes, the leaching efficiency slightly increased. This result was mainly attributed to the fact that the lead-containing components (mainly PbO in this study) easily reacted with nitric acid in the mixed solution. Especially, the surface part of PbO firstly reacted with HNO_3, and then the inner PbO was exposed and consumed by the HNO_3 in the solution.

It is also presumed that more lead ion would be leached with increasing molar ratio of HNO_3 to $Pb_{in\ the\ LART}$ (Fig.3). When the molar ratio was 1.5, the leaching efficiency of Pb at 120 min was only 67.5%, and this result was mainly attributed to the fact that the added HNO_3 (at the molar ratio of 1.5) could not entirely consume the whole PbO in the LART for the theoretical reaction molar ratio was 2. The leaching efficiency of lead was measured to be 76.7% and 82.9% at leaching time of 60 minutes, when the molar ratio was 2.5 and 3, respectively. The more nitric acid in the solution would be beneficial for the reaction with PbO from the LART, due to the easier contact between the solution and LART particles.

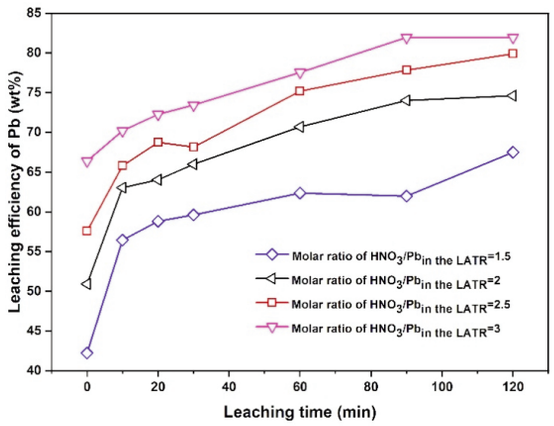

Figure 3. *Effect of molar ratios of HNO_3 to $Pb_{in\ the\ LART}$ on leaching efficiency of Pb from LART (Conditions: stirring speed of 400 rpm, 25 °C)*

The Eh-pH and Fraction phase diagrams for lead in the leaching system were shown in Fig. 4. As shown, the pH and potential of the leaching system would influence the dominant phase of lead compound in the solution. When the pH was less than 4, and the ESHE was above -0.2V, the Pb^{2+} obviously dominated in the solution. With increasing pH, the dominated phase mainly transferred into $Pb(OH)_2$.

From this above analysis result, it was easy to find that it was not essential to add oxidant or reducing agent into the leaching system, for the Pb^{2+} was dominated at a relatively large potential ranging from -0.2V to 7V. It could also be seen that the lead in the leaching system mainly existed in the dissolved state, further confirming the majority of lead was entering into the leaching solution.

However, it should be clear that small amount of lead would still be left in the residual filter cake after leaching and filtration procedure. The distribution of Pb in the stored filtrate and residual filter cake was shown in Fig. 5(a). As shown in Fig. 5(a), the proportion of lead (wt%) in the filtrate generally decreased with increasing molar ratio of HNO_3 to $Pb_{in\ the\ LART}$, due to the fact that more lead ions would be leached into the filtrate with increasing dosage of nitric acid. The sum percentage of lead in the filtrate and residual filter cake all reached more than 88% under various molar ratios, indicating that the measurement for the distribution of lead during the leaching process should be relatively accurate. This leaching process was illustrated by Fig. 5(b).

The leaching efficiency of other metal impurities

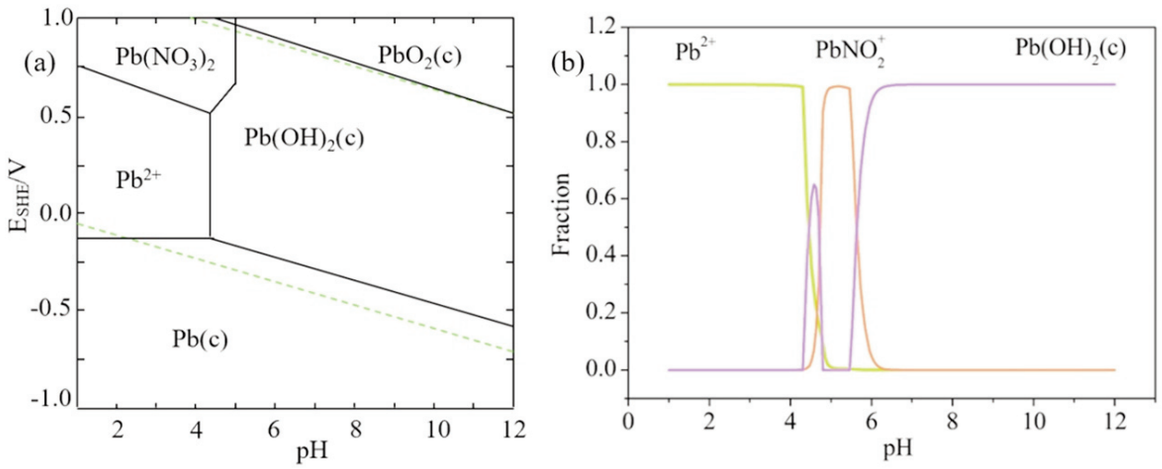

Figure 4. *Potential-pH phase diagram (a) and Fraction phase diagram (b) of Pb-HNO_3 leaching system (Conditions: 25 °C, Designed with MEDUSA software)*

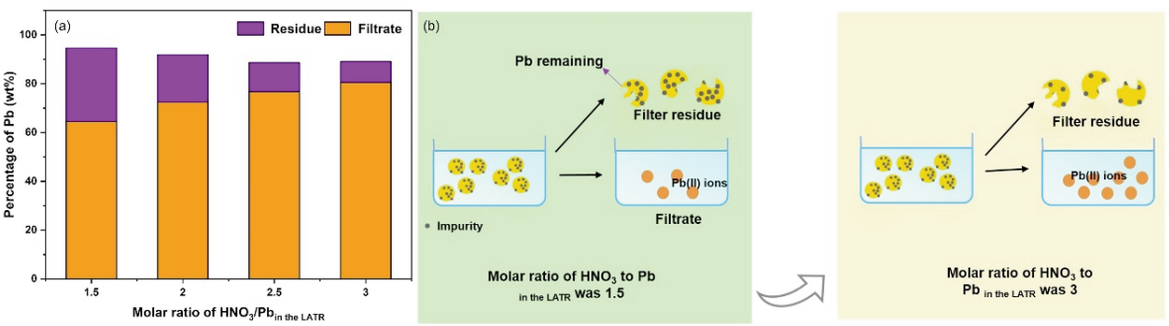

Figure 5. *(a) The molar ratio of HNO_3 to $Pb_{in\ the\ LART}$ influence on the distribution of lead in the filtrate and residual filter cake. (b) Based on the lead distribution, the schematic of lead flow during the leaching process was proposed (b). (Here, the Residue and Filtrate represented the lead leached into the filter and the lead left in the filter cake, respectively)*

including As, Cu, Fe, and Al at various molar ratio of HNO_3 to $Pb_{in\ the\ LART}$ was presented in Fig.6. The ratio of metal impurity entering into the filtrate at different molar ratio of HNO_3 to $Pb_{in\ the\ LATR}$ at the leaching time of 120 min was shown in Table S4. Table S4 shows that the most abundant element - Sn hardly reacted with the nitric acid, for its leaching efficiency was only 0.0001% at molar ratio of 1.5 and 2. Thus, the leaching efficiency of Sn was not further studied in Fig.6. As shown in Fig. 6, the ratio of As entering into the filtrate was relatively higher, and it reached up to 16% at 120 minutes at the molar ratio of 3. The leaching efficiencies of As at the molar ratio of 2.5 and 3 were relatively kept constant. At a smaller molar ratio of 1.5 and 2, the ratios of As entering into the filtrate generally decreased with increasing leaching time. The ratio of Cu entering into the filtrate generally decreased rapidly with leaching time ranging from leaching beginning to 120 min. The ratio of Cu entering into the filtrate was around 0.05~0.2% at leaching time after 20 min. The leaching efficiency of Fe generally increased with leaching time ranging from reaction beginning to 120 min, while the ratio of Fe entering into the filtrate was around 0.5~0.7% at the end of leaching process. The leaching efficiency of Al would fluctuate between 0.6~1.3% during the leaching process. Under higher molar ratio of 3, the ratio of Al in the filtrate was the highest, indicating that more Al containing compound would react with more nitric acid in the leaching system.

The Potential-pH diagram of typical impurity element including Sn, As, Fe, and Al in the leaching system could be revealed in Fig. S2. As shown in Fig. S2(a), the dominant phase for Sn element was mainly SnO_2 at pH ranging from 1 to 12 at potential of more than 0V, indicating that the Sn was merely measured in the filtrate (Table. S2). This result demonstrated that the SnO_2 could be found in the residue after leaching process. The dominant phase of As in the leaching system was more complicated, for the dominant phase of As could easily vary at varying potential. The dominant phase of Fe was transferred from Fe^{2+} ions into Fe_2O_3 (solid) with pH ranging from 1 to 12 at potential of 0V. This Potential-pH diagram result illustrated that the ratio of Fe entering into the filtrate increased with increasing molar ratio

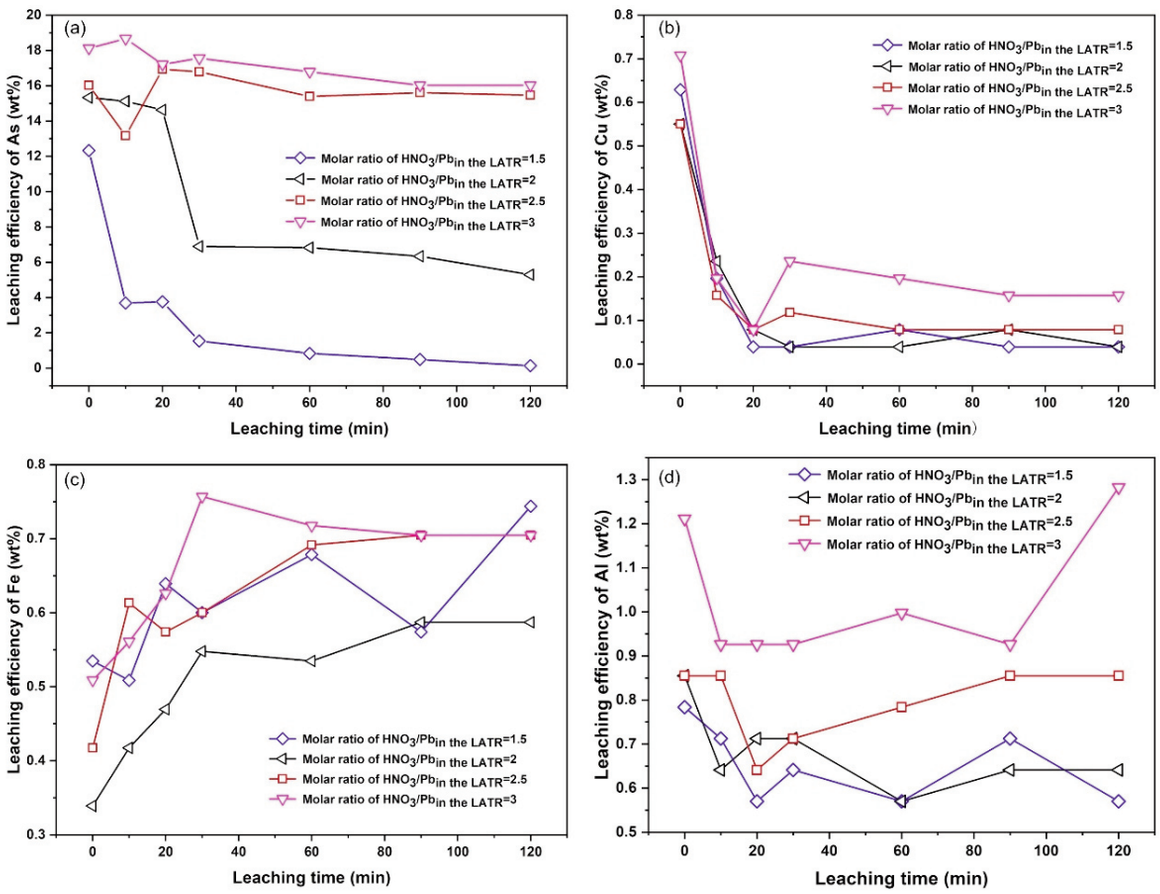

Figure 6. *Leaching efficiency of impurity elements with leaching time at different molar ratio of HNO_3 to $Pb_{\text{in the LATR}}$ (Conditions: stirring speed of 400 rpm at 25 °C): (a) As, (b) Cu, (c) Fe, and (d) Al*

of HNO_3 to $Pb_{\text{in the LATR}}$ (Fig. 6). It was obvious that the dominate phase of Al was mainly Al^{3+} ion in the solution, while the solid $Al(OH)_3$ was dominant phase at pH of higher than 4.6. Thus, with higher molar ratio of HNO_3 to $Pb_{\text{in the LATR}}$ in the leaching system, the pH decreased, which resulted in more Al^{3+} measured in the filtrate. The XRD patterns and appearance of filter residue was shown in Figure S3. The XRD patterns at various molar ratios showed that the PbO and SnO_2 were main components of the filter residue. This XRD analysis results were in accordance with the Sn in the filtrate result (Fig. 6), for part of SnO_2 was left in the residue. The appearance of the filter residue gradually changed from yellow into light yellow with increasing molar ratio of HNO_3 to $Pb_{\text{in the LATR}}$, which was attributed to the fact that less PbO was left in the residue with increasing dosage of HNO_3 in the leaching system. The weight of filter residue after leaching and filtration is shown in Tab. S3, indicating that the weight of filter residue decreased with the increasing molar ratio of HNO_3 to $Pb_{\text{in the LATR}}$. The decreasing of the filter residue was mainly the result of the fact that more PbO and element impurity in LATR reacted with more added HNO_3.

3.2. Synthesis of PbS crystal

The conversion rate of lead in the store filtrate solution (wt%) under various molar ratio of Na_2S to Pb in the filtrate was presented in Fig. 7(a). As shown, the conversion rate of lead increased with increasing molar ratio of Na_2S to Pb in the filtrate ranging from 0.75 to 1.5. The reaction between the sodium sulfide and the lead nitrate in the filtrate was presented by Eq. 3, indicating that the theoretical molar ratio of sodium sulfide to lead nitrate was 1:1. With more added sodium sulfide, the lead ions in the stored filtrate would be easier to contact and react with the sulfur ion in the system, while more amount of PbS crystal would be generated, as illustrated by Fig. 7(b). The appearance of the synthetic PbS crystal product was shown in Fig. 7(I–IV), while the prepared PbS crystal products were all black powders, further confirming the existence of PbS. From the appearance of products, not obvious appearance difference for PbS crystal was observed at different molar ratios.

$$Pb(NO_3)_2 + Na_2S \rightarrow PbS + 2NaNO_3 \qquad (3)$$

The XRD patterns of the generated PbS crystal at various molar ratios of Na_2S to Pb in the filtrate was shown in the Fig. 8(a). The XRD results indicated that all of the generated powders were pure PbS crystal (PDF: 03-0614) at various molar ratios, indicating that the prepared PbS crystal was of high purity. The

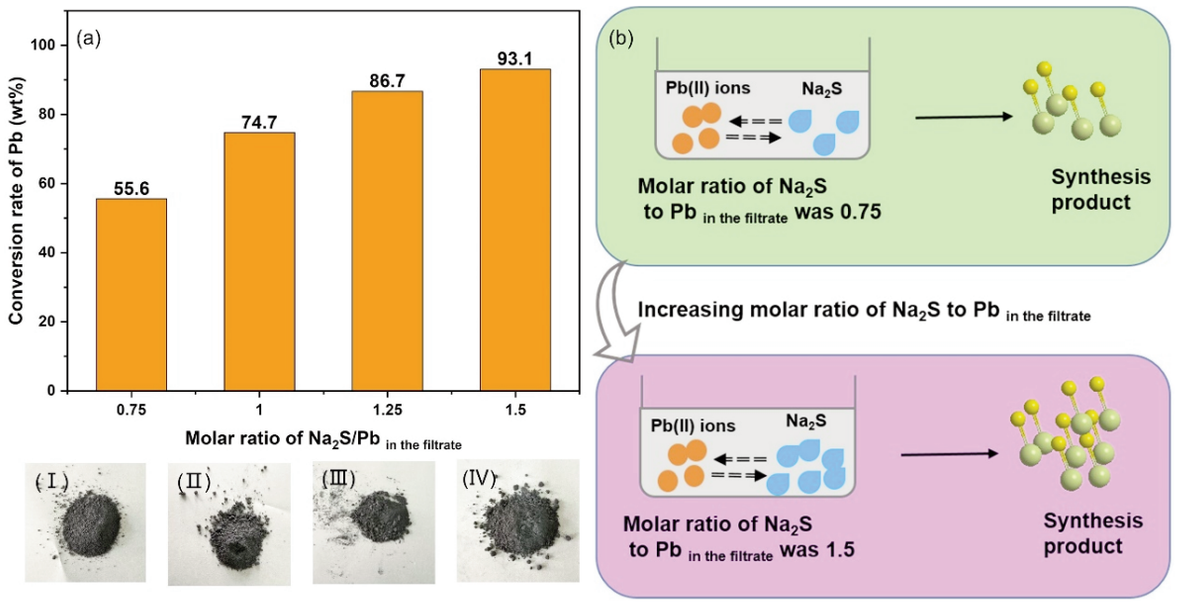

Figure 7. *The conversion of lead in the filtrate to the PbS crystal (Conditions: stirring speed of 300 rpm, and temperature of 25 °C): (a) the conversion rate of lead at different molar ratio of Na_2S to $Pb_{in\ the\ filtrate}$; (b) Proposed model for the synthesis of PbS crystal; (I–IV) the appearances of the products for the synthesis procedure at molar ratio of 0.75, 1, 1.25 and 1.5, respectively*

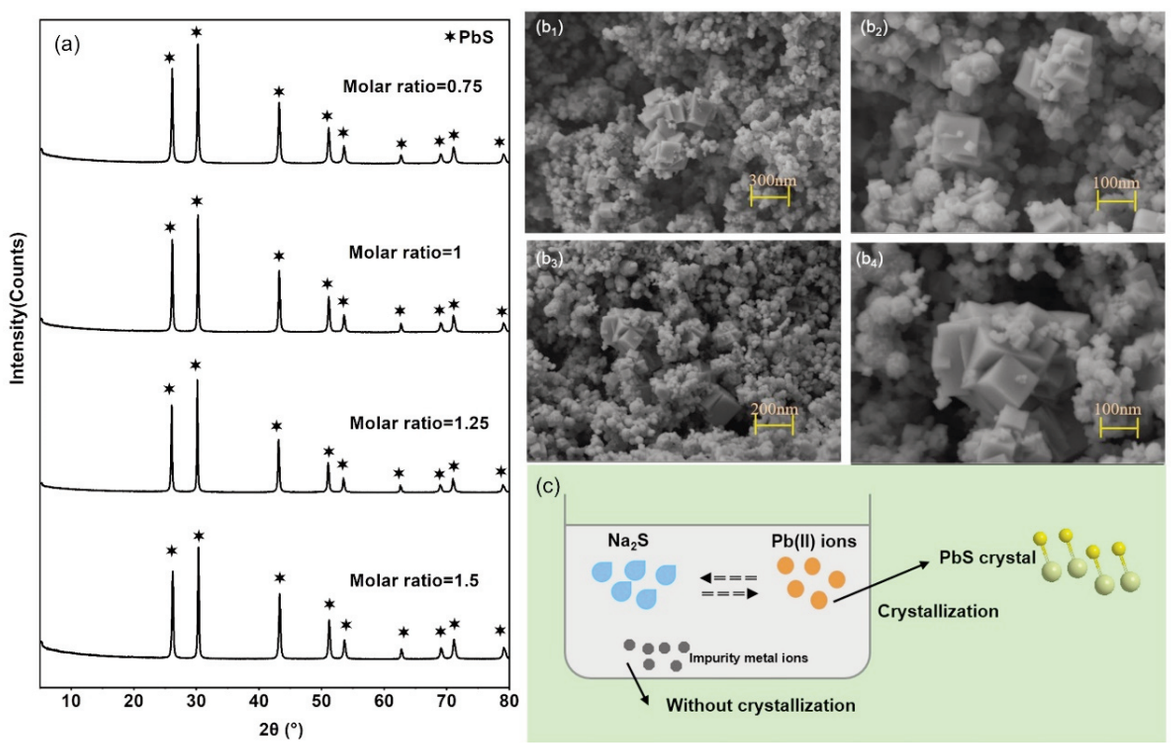

Figure 8. *The material characterization of the prepared crystal products (Conditions: stirring speed of 300 rpm, temperature at 25°C): (a) the XRD patterns; (b) the SEM diagrams ((b1, b2) the molar ratio of Na_2S to Pb in the filtrate=0.75, (b3, b4) the molar ratio of Na_2S to $Pb_{in\ the\ filtrate}$=1.5); (c) the proposed model for the separation of Pb ions from the impurities*

SEM images of PbS crystal synthesized at molar ratio of 0.75 and 1.5 were shown in Fig. 8(b1)-(b4). As shown, not obvious difference was observed between the products at different molar ratio of Na_2S to $Pb_{in\ the\ filtrate}$. The prepared PbS crystal was mainly rendering square blocks with varying dimension ranging among 20 and 100 nm, indicating the prepared PbS powders were mainly nano-sized materials. The crystallization process would be beneficial to the separation of other element from the lead containing crystal, due to their different crystallization performance as shown in Fig. 8(c) [28, 29].

It could be revealed that most part of lead was transferred into the PbS crystal product, while only a small part of lead was left in the filtrate. The lead distribution in the PbS crystal and filtrate was shown in Fig.S4. As shown in Fig.S4, the amount of lead in the synthetic product generally increased with increasing molar ratio of Na_2S to Pb in the filtrate, which was attributed to the fact that more lead ions would contact and react with sufficient sulfur ions with the increasing dosage of sodium sulfide reagent. The percentage of lead in the synthetic product and filtrate would be summed for more than 88% under various molar ratios as presented in Fig.S4. The sum percentage of lead was maximum when the molar ratio of Na_2S to Pb in the filtrate was 1.5, which could attain to 94.5%.

4. Conclusion

The PbS crystal was successfully synthesized through this high-speed leaching and recrystallization method. The leaching efficiency of lead increased with increasing molar ratio of HNO_3 to $Pb_{in\ the\ LATR}$, which reached up to 82.9% at the molar ratio of 3. The main metal impurities in the leaching process were Sn, As, Cu, Fe, and Al. The ratio of As, Cu, Fe, and Al entering into the filtrate increased when the molar ratio of HNO_3 to $Pb_{in\ the\ LATR}$ increased from 1.5 to 3, while the ratio of Sn entering into the filtrate was only 0.002% at the molar ratio of 3. The yield of PbS crystal increased with increasing molar ratio of Na_2S to $Pb_{in\ the\ filtrate}$, which reached up to 93.1% at the molar ratio of Na_2S to $Pb_{in\ the\ filtrate}$ of 1.5. As shown in the XRD patterns of the product, the product was relatively pure crystal of PbS. The method could provide a green route for the efficient recovery of lead from waste lead ash at room temperature, which would not generate lead particles and high energy consumption. In the future recycling process, the recovery of Sn and other precious metals should be further considered.

Acknowledgments

The authors gratefully thank the support of the Natural Sciences Foundation of China (grant No. 52000163), the Key Project of Natural Science Foundation of China–Xinjiang Joint Fund (grant No. U1803241) and the Natural Sciences Foundation of China (grant No. 51779230). The authors also thank the Natural Science Foundation of Henan Province (grant No. 202300410423).

References

[1] M. Y. Sun, J. S. Mao, J. Ind. Ecol., 22 (1) (2018) 155-165.

[2] W. Liu, Z. J. Cui, J. P. Tian, et al., J. Clean. Prod., 205 (2018) 86-94.

[3] L. Y. Sun, C. Zhang, J. H. Li, et al., J. Environ. Manage., 183 (1) (2016) 275-279.

[4] X. Tian, Y. Gong, Y. F. Wu, et al., Resour. Conserv. Recy., 93 (2014) 75-84.

[5] W. Zhang, J. K. Yang, X. F. Zhu, et al., J. Chem. Technol. Bito., 91 (3) (2016) 672-679.

[6] D. L. Yang, Y. Q. Yin, X. T. Ma, et al., Int. J. Life. Cycle. Ass., 24 (8) (2019) 1533-1542.

[7] L. Q. Wu, M. P. Taylor, H. K. Handley, Sci. Total. Environ., 599 (2017) 1233-1240.

[8] M. Albitar, M. S. M. Ali, P. Visintin, et al., Constr. Build. Mater., 83 (2015) 128-135.

[9] B. R. Zhang, W. X. Zhou, H. P. Zhao, et al., Waste. Manage., 50 (2016) 105-112.

[10] G. Uzu, S. Sobanska, G. Sarret, et al., J. Hazard. Mater., 186 (2-3) (2011) 1018-1027.

[11] K. H. Gu, W. H. Li, J. W. Han, et al., Sep. Purif. Technol., 209 (2019) 128-135.

[12] R. Kermer, S. Hedrich, S. Bellenberg, et al., Hydrometallurgy., 168 (2017) 141-152.

[13] W. N. Oehmig, J. G. Roessler, J. Y. Zhang, et al., J. Hazard. Mater., 283 (2015) 500-506.

[14] X. M. Dou, F. Ren, M. Q. Nguyen, et al., Renew. Sust. Energ. Rev., 79 (2017) 24-38.

[15] X. Tian, Y. F. Wu, P. Hou, et al., J. Clean. Prod., 144 (2017) 142-148.

[16] W. Zhang, G. Tang, X. Q. Xiang, et al., Chinese. J. Chem. Eng., 27 (7) (2019) 1674–167.

[17] C. S. Chen, Y. J. Shih, Y. H. Huang, Waste. Manage., 52 (2016) 212-220.

[18] W. Zhang, J. K. Yang, X. Wu, et al., Renew. Sust. Energ. Rev., 61 (2016) 108-122.

[19] P. Xing, C. H. Wang, L. Wang, et al., Hydrometallurgy., 189 (2019) 105134.

[20] M. H. Li, J. K. Yang, S. Liang, et al., J. Power. Sources., 436 (2019) 226853.

[21] A. L. Ji, F. Wang, W. J. Luo, et al., Lancet., 377 (2011) 1474-1476.

[22] Y. Liu, M. X. Liu, D. Q. Yin, et al., Nanoscale., 11 (2019) 136-144.

[23] K. Liu, S. Liang, J. X. Wang, et al., Sustain. Chem. Eng., 6 (12) (2018) 17333-17339.

[24] K. Liu, J. H. Yang, S. Liang, et al., Environ. Sci. Technol., 52 (4) (2018) 2235-2241.

[25] R. Torres, G. T. Lapidus, Waste. Manage., 60 (2017) 561-568.

[26] R. Zárate-Gutiérrez, G. T. Lapidus, Hydrometallurgy., 144 (2014) 124-128.
[27] G. Eriksson, Anal. Chim. Acta., 112 (4) (1979) 375-383.
[28] S. Kull, L. Heymann, A. B. Hungria, et al., Chem. Mater., 31 (15) (2019) 5646-5654.
[29] W. Meng, W. Y. Yuan, Z. B. Wu, et al., Powder. Technol., 347 (2019) 130-135.

Suplementary File

Table S1. *Leaching experimental material dosing scheme*

No.	Dosage of LATR		Mole of HNO_3 to $Pb_{in\ the\ LATR}$	Dosage of nitric acid		
	Mass (g)	Mole (mol)		Mole of HNO_3 (mol)	Adjusted concentration of HNO_3 (mol/L)	Volume of HNO_3 (mL)
1	50	0.1824	1.5	0.2736	0.6	456
2			2	0.3648	0.8	
3			2.5	0.456	1	
4			3	0.5472	1.2	

Table S2. *PbS crystal synthesis experimental material dosing scheme*

NO.	Leaching filtrate				Dosage of sodium sulfide	
	Volume (mL)	Mole of $Pb_{in\ the\ filtrate}$ (mol)	Mass of $Pb_{in\ the\ filtrate}$ (g)	Molar ratio of $Na_2S/Pb_{in\ the\ filtrate}$	Mole (mol)	Mass (g)
I	50	0.0179	3.6967	0.75	0.0134	3.2244
II				1	0.0179	4.2992
III				1.25	0.0224	5.3739
IV				1.5	0.0269	6.4535

Table S3. *Mass of filter residue with different molar ratio of HNO_3 to $Pb_{in\ the\ LATR}$*

Molar ratio of $HNO_3/Pb_{in\ the\ LATR}$	1.5	2	2.5	3
Filter residue weight (g)	20.88	17.07	15.75	14.85
Percentage of filter residue/LATR (wt%)	41.76	34.14	31.5	29.7

Table S4. *Ratio of metal impurity entering into the filtrate under different molar ratio of HNO_3 to $Pb_{in\ the\ LATR}$ at leaching terminal of 120 min*

Metal impurity	Initial mass of metal impurity in 50 g of LART (mg)	Leaching process: various molar ratio of HNO_3 to $Pb_{in\ the\ LATR}$	Amount of metal impurity entering into the filtrate (mg)	Ratio of meal impurity entering into the filtrate (wt%)
Sn	3619.25	1.5	0.0036	0.0001
		2	0.0036	0.0001
		2.5	0.0072	0.0002
		3	0.0072	0.0002
As	654.5	1.5	0.91644	0.14
		2	34.6938	5.3
		2.5	101.2	15.46
		3	104.87	16.02
Fe	34.95	1.5	0.2586	0.74
		2	0.2062	0.59
		2.5	0.2447	0.7
		3	0.2447	0.7
Cu	11.6	1.5	0.0046	0.04
		2	0.0046	0.04
		2.5	0.0092	0.08
		3	0.0184	0.16
Al	6.4	1.5	0.0365	0.57
		2	0.041	0.64
		2.5	0.055	0.86
		3	0.0819	1.28

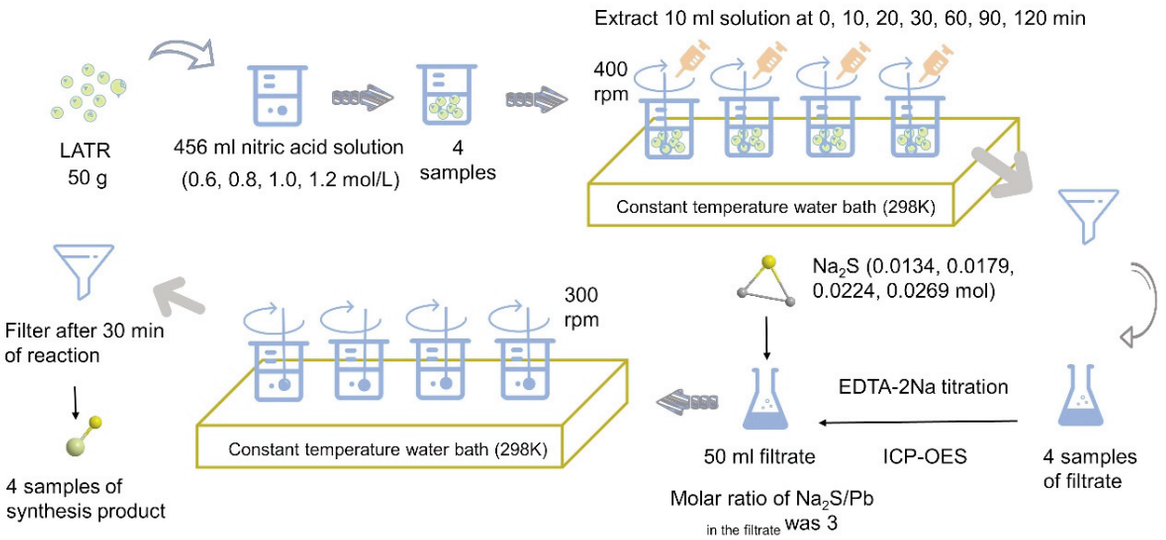

Figure S1. *Experimental process diagram of LATR leaching and PbS crystal synthesis*

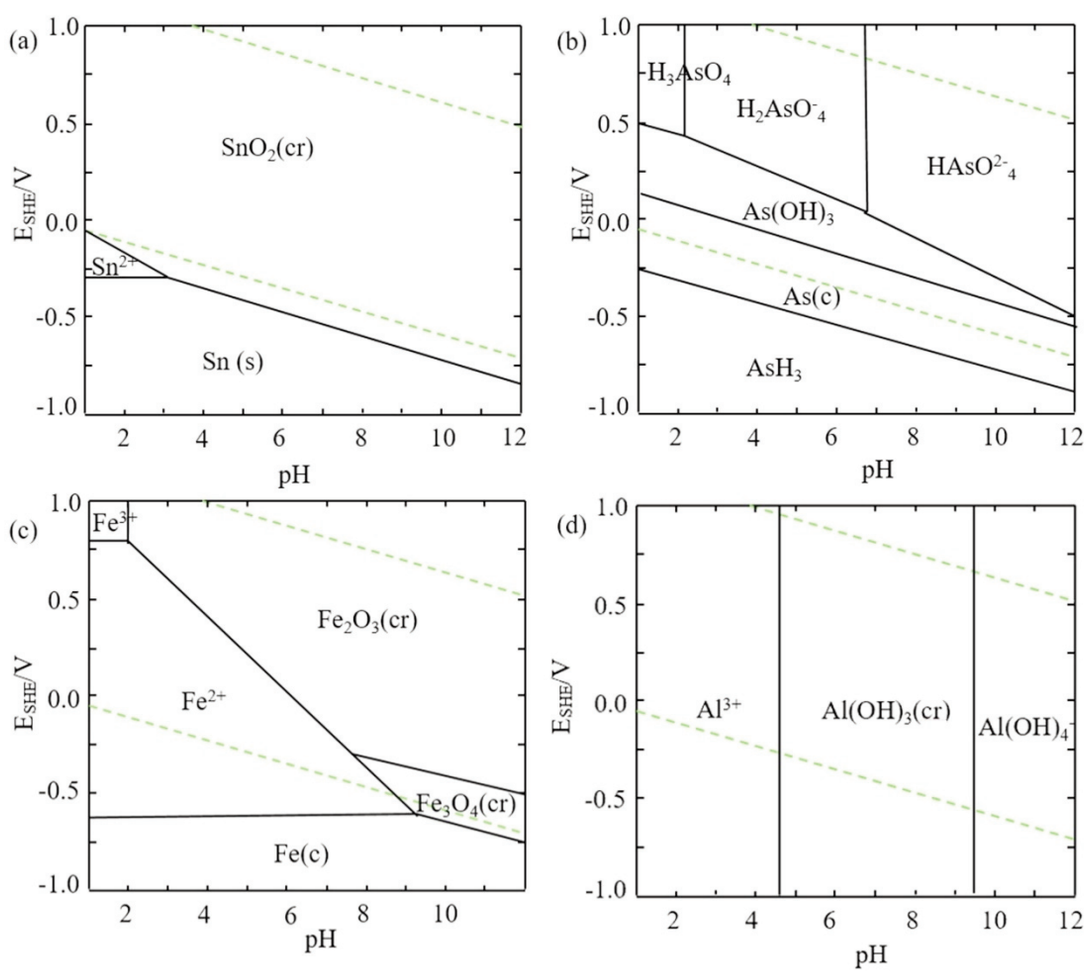

Figure S2. *Potential-pH phase diagrams for main metal impurities in the presence of nitric acid in leaching system: (a) Sn; (b) As; (c) Fe; (d) Al, at 25 °C. Designed with MEDUSA software*

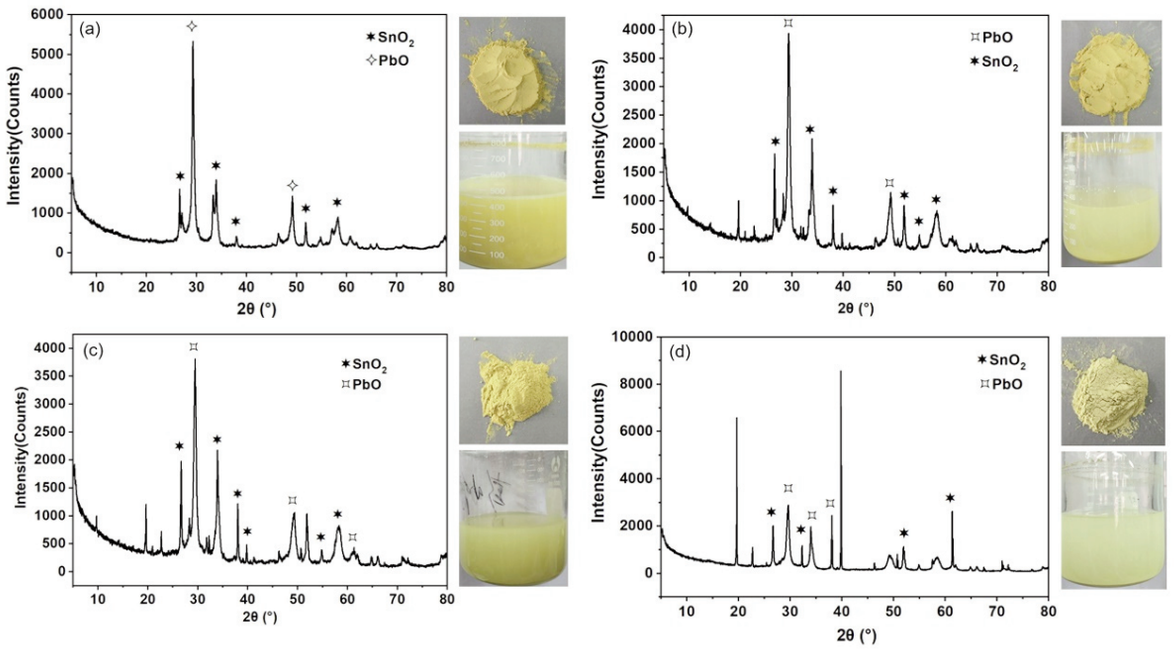

Figure S3. *XRD patterns, real picture of leaching residues and post-reaction solution with various molar ratio of HNO_3 to $Pb_{\text{in the LATR}}$: (a) Molar ratio of 1.5; (b) Molar ratio of 2.0; (c) Molar ratio of 2.5; (d) Molar ratio of 3.0*

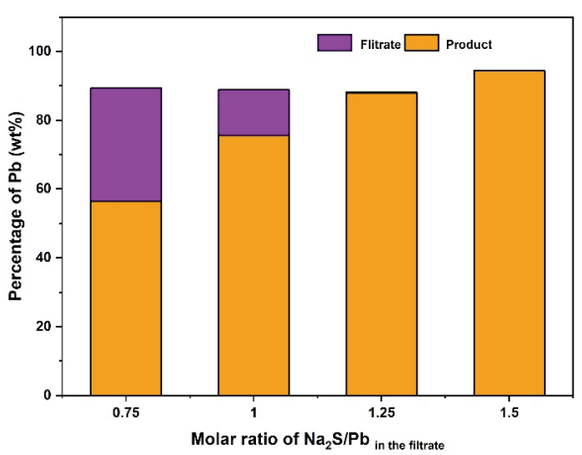

Figure S4. *The molar ratio of Na_2S to $Pb_{\text{in the filtrate}}$ influence on the percent of lead (wt%) in the product and filtrate. Here, the Filter and Product was representing the lead left in the filter and transferred into the product, respectively*

EDTA-2Na Testing Method

3 mL of filtrate was pipetted into a 250 mL erlenmeyer flask and diluted with water to about 90 mL. The pH of the solution was adjusted to 5 ~ 6 with 1 : 1 ammonia water, while 5 mL of 20% sodium acetate solution and 5 mL of 20% hexamethylenetetramine were used as buffer solutions to stabilize the pH. Three drops of 0.5% xylenol orange indicator were added and shaken well. At this time, the solution was purple - red. Standard solution was titrated with the 0.05 mol/L EDTA-2Na after calibration until the solution changed from purple - red to bright yellow. Record the amount of EDTA-2Na standard solution as v4E, then the lead ion concentration was shown as Eq. (S1):

$$m_4 = c_4 \times v_{4E} \times m_r / v_4 \quad \text{(S1)}$$

Where m_4 is the concentration of the lead ion, g/L; c_4 is the concentration of the EDTA-2Na, mol/L; v_{4E} stands the dosage of EDTA-2Na, mL; m_r is the relative molecular weight of lead, g/mol, 207.1; v_4 is the filtrate volume, mL, take 3 mL at this experiment.

Determination of the impurity elements in the LATR

LATR materials (0.2 g) was placed in a beaker (50 mL), then 15.0 mL of aqua regia into the beaker was added. The slurry containing LATR materials and aqua regia was heated at 200 °C until no obvious particle solid was observed in the slurry. The diluted nitric acid solution (3% wt) was added into the slurry until the volume reached up to 30 mL, then it was cooled down to room temperature. The slurry was finally filtered through microporous filter membrane and diluted into a 50 mL colorimetric tube. The concentration of impurities in the filtrate was eventually determined by ICP-OES 5100 (Keysight Technologies).

EFIKASAN I EKOLOŠKI PRIHVATLJIV NAČIN ZA DOBIJANJE PBS KRISTALA IZ PEPELA SA SADRŽAJEM OLOVA NASTALOG TOKOM LUŽENJA I POSTUPKA REKRISTALIZACIJE

Y.-K. Feng [a,b], X.-Q. Peng [a], H.-H. Shi [a], W. Zhang [a,c,d,e*], Q.-T. Zuo [b,c,d,e#]

[a] Fakutltet za ekologiju i životnu sredinu, Univerzitet u Džengdžou, Džengdžou, Henan, Kina
[b] Fakultet za inženjerstvo očuvanja vode, Univerzitet u Džengdžou, Džengdžou, Henan, Kina
[c] Međunarodna laboratorija za simulaciju ciklusa vode i zaštitu životne sredine u Henan provinciji, Džengdžou, Kina
[d] Glavna laboratorija za vodne resurse i životnu sredinu u Džengdžou, Džengdžou, Kina
[e] Institut „Žuta reka“ za zaštitu životne sredine i koordinaciju regionalnog razvoja, Džengdžou, Kina

Apstrakt

U ovom radu je ispitivana sinteza PbS kristala visoke čistoće iz pepela sa sadržajem olova koji je dobijen tokom postupka uklanjanja kalaja iz pepela. Pepeo je prvo izložen postupku luženja u prisustvu azotne kiseline da bi se dobio rastvor olovo nitrata. PbS kristal je pripremljen mešanjem rastvora olovo nitrata i natrijum sulfida na sobnoj temperaturi (25 °C). Ispitan je uticaj molarnog odnosa HNO_3 i $Pb_{u\ pepelu}$ na efikasnost luženja Pb, i dokazano je da efikasnost luženja Pb dostiže 82,9% kada je molarni odnos 3. Odnos za luženje As, Cu, Fe i Al se povećavao sa povećanjem molarnog odnosa HNO_3 i $Pb_{u\ pepelu}$, dok je 99,99 mas% Sn ostalo u talogu. Tokom postupka generisanja PbS kristala iz rastvora za luženje, prinos kristala se povećao kada se povećao molarni odnos Na_2S i $Pb_{u\ filtratu}$. Prinos PbS kristala može dostići i 93,1% kada je molarni odnos 1,5. Sve u svemu, ovaj metod se pokazao kao efikasan i ekološki prihvatljiv način za sintezu PbS kristala visoke čistoće direktno iz običnog otpada koji sadrži olovo iz rude olova ili indirektno iz topionice.

Ključne reči: *Pepeo sa sdržajem olova; PbS kristali; Luženje; Rekristalizacija; Dobijanje; Ekološki prihvatljivo*